이학석사 학위논문

Strong Absorption of Lactose Molecule inside Terahertz Nano-slot Antenna

테라헤르츠 나노슬랏 안테나 안의 락토즈 분자에서의 강한 흡수

2012 년 8 월

서울대학교 대학원

물리천문학부

이 지 예

Strong Absorption of Lactose Molecule inside Terahertz Nano-slot Antenna

by

Jiyeah Rhie

Supervised by

Prof. Dai-Sik Kim

A Dissertation

Submitted to Faculty of Seoul National University

In Candidacy for the Degree of Master

August 2012

Department of Physics and Astronomy

Graduate School

Seoul National University

Strong Absorption of Lactose Molecule inside Terahertz Nano-slot Antenna

지도 교수 김 대 식

이 논문을 이학석사 학위논문으로 제출함
2012년 8월

서울대학교 대학원
물리천문학부
이 지 예

이지예의 이학석사 학위논문을 인준함
2012년 6월

위 원 장 _____ (인)

부위원장 _____ (인)

위 원 _____ (인)

Abstract

Absorption of terahertz (THz) electromagnetic waves through lactose molecules (α-lactose monohydrate) inside a single nano-slot antenna is investigated. Recent studies have shown that lactose molecules have an absorption frequency at 0.53 THz. Since nano-slot antenna also has a resonance behavior, we designed the antenna to have same resonance of lactose molecules. When the molecules are inside the field enhancement of nano-slot antenna, absorption coefficient and absorbed energy per molecule shows an increase 200,000% and 5,000,000% each. In result, we suggest nano-slot antenna as a tool for detecting materials sensitively with its absorption resonance.

Keywords : terahertz, lactose, nano-slot antenna, absorption

Student Number : 2010-23151

Contents

Chapter 1

Introduction

Molecular spectroscopy has been a topic of interest for interdisciplinary research for the detection, identification, and the dynamitic study of single molecules[5,6,11-17]. Since the vibrations depend on the particular molecular structure[19,20], the energy spectrum of molecular vibrations can lead to an unambiguous characteristic fingerprint for the chemical composition of a sample[11]. Infrared (IR) waves, which the frequency range is approximately 1 to 400 terahertz (THz), can provide the information of intramolecular vibrational modes[19]. However, IR spectroscopy, like Raman scattering, itself has shown relatively low absorption and low scattering cross-sections of molecules for analyzing materials[11,16]. In 1974 it was reported that the Raman scattering cross-section can be considerably increased if the molecules are adsorbed on roughened metal surfaces[11]. Rough metal surfaces are usually formed by evaporating metallic thin films, which consists of metal particles much smaller than the wavelength of light. Electric field associated with the incident infrared radiation is enhanced via the excitation of localized plasmon of the particles, yielding the absorption enhancement. The examples of this surface enhanced method are surface enhanced Raman spectroscopy (SERS) [11,16], and surface enhanced IR absorption spectroscopy (SEIRA) [13,14]. These methods were used for single molecule detection by coupling single molecules to metallic nanoparticles. With this method, the molecular

vibrational modes of the molecules have been mainly investigated in their solid form by, for example, pressing powders into pellets about few milligrams[6,19].

Even though the bulk of SERS and SEIRA were used for research, there were limitations. Because of their random nature and uncontrolled geometries, signal enhancement factors were limited to 10~ 100 ranges[12]. Furthermore, they caused poor spectral overlap between plasmonic resonances and the molecular vibrational modes of interest[12,15,17]. Collectively enhanced IR absorption spectroscopy (CEIRA) was introduced to increase the signal enhancement factors by using optical antennas[12]. Engineered optical antennas have the ability of sensing chemicals and biomolecules with their spectral selectivity. Their resonant response can be accurately tuned to that of the vibrational modes of the target materials because they can support spectrally well-defined resonances due to the strong local fields[15,17].

H. Altug *et al.* shown the absorption enhancement factor of 10^4~10^5 by using nano-rod antenna arrays. H. Altug and G. Shevets *et al.* improved the sharpness of the absorption resonance by introducing plasmonic Fano-resonant asymmetric metamaterials (FRAMMs) [15] as an optical antenna. Fano-like optical antenna, FRAMMs, can simultaneously probe structural and binding characteristics of biomolecular interactions by using the full information content of the

biomolecules' frequency-dependent infrared response. The reason is that they have a spectrally narrow response and high local field concentration. Owing to these properties, optical antennas have emerged as a powerful photonic platform for sensing and identifying the materials. However, these optical antennas with positive structure have an ambiguous volume of containing molecules. These structures give lack of information for getting quantitative interpretation. Therefore, we used nano-slot antenna as a negative structure to fix the volume.

While IR region includes the information of intramolecular vibrational modes, THz waves consists intermolecular vibrational modes. Although researchers and studies have analyzed the characteristics of materials with intramolecular vibrational modes, there are also chemical materials, explosives (RDX, TNT), and biomolecules that can be identified with intermolecular vibrational modes. Lactose is also a representative material used for fingerprint or THz spectra because of its absorbed resonance happens in THz region (0.1 THz~ 10 THz)[5,6,24]. THz spectroscopy enables the detection and identification of molecules or materials that have strong absorption in the THz region.

In this paper, we used the engineered optical antenna that matches with the absorption resonance of lactose molecule. Since electric field and magnetic field inside of nano-slot antenna are both fully exploded,

we choose nano-slot antenna as an optical antenna which has negative structure. The fixed volume that contains lactose molecules enables us to study the effect of nano-slot antenna by analyzing lactose molecules' absorption coefficient and absorption energy per molecule.

Chapter 2

Terahertz Nano-Slot Antenna

2.1. Single Rectangular Hole

Both the square hole and circular hole are poor antennas and their singularities are of an integrable kind, which limits the field enhancements. One way to dramatically increase the field enhancement is to make the aperture a strongly asymmetric rectangle, which support a well-defined transmission resonance for light polarized along its short side.

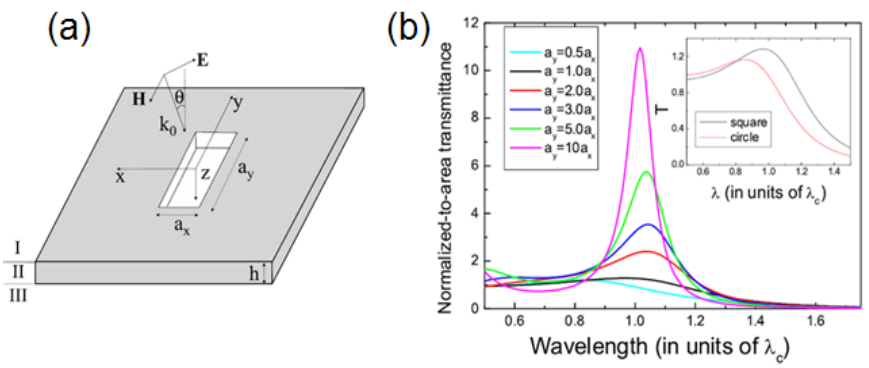

Fig.1. (a) Schematic of a single rectangular hole of sides a_x and a_y perforated on a metal film of thickness h. (b) Normalized-to-area transmittance versus wavelength (in units of the cutoff wavelength $\lambda_c = 2a_y$), for a normal incident plane wave impinging on a rectangular hole, for different rations a_y/a_x (adopted from ref.[1])

F. J. Garcia-Vidal *et al.* have shown numerically that a single rectangular hole exhibits strong transmission resonances near their cut-off wavelengths[1]. Fig. 1 (a) shows schematically the system: a rectangular hole of sides a_x and a_y perforated on a metallic film of

thickness h. The structure is illuminated by a p-polarized light and the metal is treated as a perfect electrical conductor (PEC), a good approximation in the THz frequency regime. Fig. 1 (b) depicts the calculated normalized-to-area transmission spectra for rectangles in which the aspect ratio (a_y/a_x) is varied between 1 (square hole) and 10. The thickness of the metallic film is fixed in all cases at $h = a_y/3$. As the ratio a_y/a_x is increased, a transmission peak develops close to the cut-off wavelength ($\lambda_c = 2a_y$), with increasing maximum transmittance and decreasing line width. The physical origin of the transmission resonances appearing at $\lambda_{res} = \lambda_c$ stems from the excitation of a Fabry-Perot resonance in which the propagation constant is zero. An analytical approximation for the transmittance at resonance T_{res} can be obtained by

$$T_{res} \approx \frac{3}{4\pi}\frac{{\lambda_{res}}^2}{a_x a_y} \approx \frac{3}{\pi}\frac{a_y}{a_x} \quad (1)$$

It is noted that the transmission cross-section of a rectangular hole is given by the square of the long (a_y) sides of the rectangle at the resonance, so that it is proportional to ${\lambda_{res}}^2$, $\sigma_{res} \approx \frac{3}{4\pi}{\lambda_{res}}^2$. A close analogy is found in a bound charges with losses only though radiation, whose resonant cross-section is also proportional to ${\lambda_{res}}^2$, $\sigma_{res} \approx \frac{3}{2\pi}{\lambda_{res}}^2$. The cross-section of the rectangle is half this value because we are only looking at the transmittance, not reflection. The electric

field enhancement has also the form resembling Eq. (1), because both energy and amplitude enhancements are essentially the same because the magnetic field amplitude is almost identical to the incident one. The electric field enhancement can be verified by near-field imaging experiments. While other techniques enables to measure the amplitude and phase at discrete THz frequencies, time-domain spectroscopy can additionally measure the electric field as a function of time, and obtain the spectrum by a Fourier transform of the time domain data. THz time-domain spectroscopy (THz-TDS) is used to measure the far field enhancement for various samples.

In 2007, M. A. Seo *et al.*[2] experimentally verified the occurrence of a large field enhancement through the rectangular hole in the THz frequency range, using terahertz Fourier-transform near-field imaging with ~λ/100 resolution. They could measure the component parallel to the short side of rectangle, i. e. the main near field component. Fig. 2 (a), (b), and (c) are the images for samples with a_x =100, 50 and 10 μm, respectively for a fixed length of a_y =300 μm at 0.2 THz, which is the approximated resonant frequency. These figures show that the near-field amplitude becomes proportionally stronger as the rectangular hole becomes narrower. The field enhancement increases with the increasing aspect ratio the rectangular hole, a_y/a_x, and therefore with decreasing width of the rectangle (Fig. 2 (d)). Fig. 2 (e) shows that the area-

integrated field amplitude remains nearly constant for different widths of rectangle. It strongly suggests that the same amount of energy passes through a narrow rectangular hole, confirming the funneling of energy in the near-field.

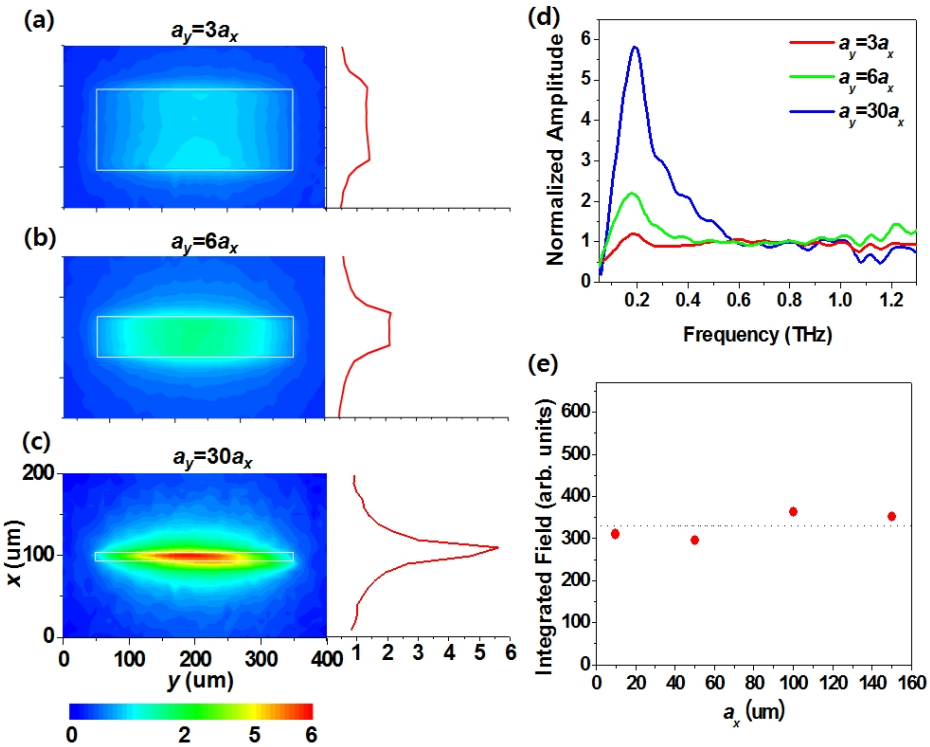

Fig.2. (a) x-component of electric near-fields around single rectangles of different widths for fixed length, grown on top of the electro-optic (EO) crystal (GaP). The plotted images are shown for (a), a_x=100 μm, (b), a_x=50 μm, and (c), a_x =10 μm, respectively. The length is fixed at 300 μm. The line on the right side is cutting through the center of the hole. The spectra at the center of the rectangle for various aspect ratios are shown. The integrated amplitude over the area of the rectangle versus the width of the rectangle is shown (e)(adopted from ref.[2]).

2.2. Nano-Antennas

In the previous section, the rectangular hole structures had micron-sized widths. In this regime, it has been shown, theoretically and experimentally, that the field enhancement inside holes increase as the width decreases. A natural question is whether this field enhancement will keep going up as we decrease the width into the nanoscale.

In this section, we will image long rectangular holes with nano-sized widths, called THz nano-antennas or THz nano-resonators. Previously, our group has shown that this structure can induce field enhancement in the range of a few hundred for the fundamental resonance, estimated by the Kirchhoff integral formalism[18]. These THz nano-antennas with a striking aspect ratio funnel THz electromagnetic waves through, accompanied by a large field enhancement unavailable for micron-sized width. THz nano-antennas with giant field enhancement open a strong possibility of potential applications, such as broadband field enhancement and nonlinear devices, filter, detectors, and active switching devices[4].

2.2.1. Nano-Slit

In 2009, a 10^3 field enhancement inside a very narrow slit has been demonstrated by measuring the transmitted far field in the THz regime[3]. Fig. 3 (a) presents a schematic of experiment set-up. The sample consisted of a nano-slit (width, w =70 nm) fabricated using a focused ion beam on the 60 nm-thick gold film. To obtain normalized transmitted amplitude through the nano-slit, they performed THz far field TDS with single-cycle terahertz source generated from a 2 kV/cm biased semi-insulating GaAs emitter. The emitter is illuminated by a femtosecond Ti:sapphire laser pulse train of a center-wavelength 780 nm, a 76 MHz repetition rate and a 130 fs pulse width. An EO sampling method was used to detect the transmitted terahertz waves in the time domain, in which an optical probe pulse undergoes a slight polarization rotation by the synchronized terahertz beam in a (110) oriented ZnTe crystal, detecting the horizontal electric field.

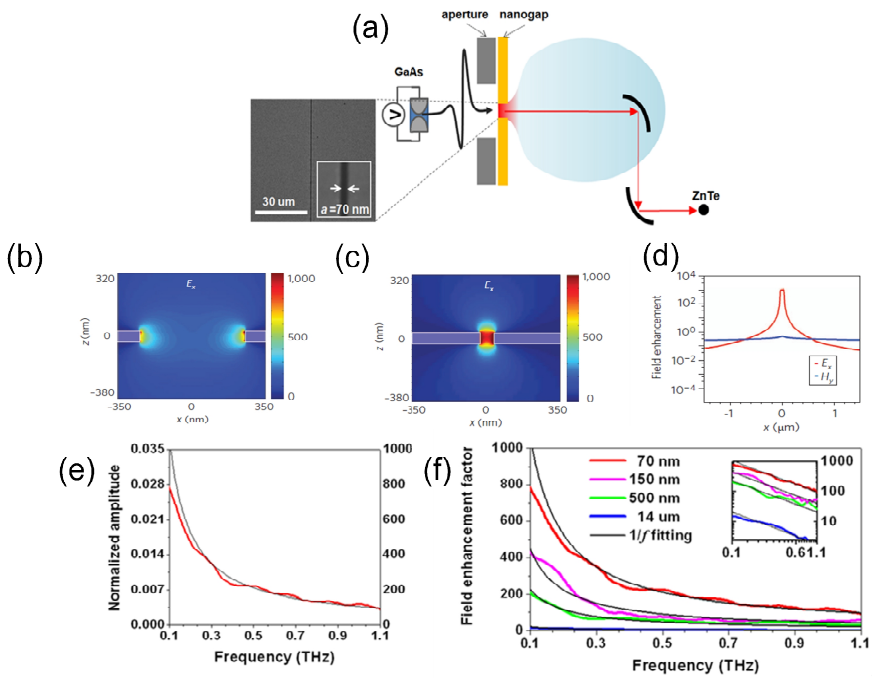

Fig.3. (a) An scanning electron microscope (SEM) image of a 70 nm-width nanogap perforated on gold film and terahertz time-domain spectroscopy using EO sampling for detection of far-field transmitted amplitudes. (b) Simulated horizontal electric field around 500 nm - width at 0.1THz. (c) Horizontal electric field around 70 nm-width are shown in FDTD analysis. (d) Cross-sectional plot of the horizontal electric and magnetic fields at the exit side. (e) Normalized amplitude and field enhancement shown on the right axis. (f) Field enhancement through samples with various gap widths: a =70, 150, 500 nm and 14 μm, where h =60, 150, 60 nm and 17 μm, respectively (adopted from ref.[3]).

The transmitted far-field amplitude is connected to the enhanced near-field amplitude at the gap through Kirchhoff integral formalism. Fig. 3 (e) shows the normalized amplitude, $\alpha(\omega)$, for the nano-gap sample, reaching 2.7% at the lowest frequency of 0.1 THz. The nanogap-to-aperture area ratio, β = width(nanogap)/width(aperture), is only 0.0035%= 70 nm/2 mm. From these results, they could obtain the near-field enhancement inside the gap, by a factor of 800. They also proved that the electric field increases with decreasing slit width (Fig. 3 (f)).

To understand these phenomena occurring near the nano-slit, a two-dimensional finite-difference time-domain (FDTD) analysis was carried out. Fig. 3 (b) and (c) show an increasing field enhancement with a decreasing gap beyond the skin depth regime. It is in good agreement with the experimental results. While the horizontal electric field at the gap is orders of magnitudes stronger, the magnetic field stays mostly on the order of 1, but with a very small curvature resulting in an enormous curl.

2.2.2. Nano-Slot

H. R. Park *et al.* present a giant field enhancement of the THz electric field through THz nano-antennas which are hundreds of microns in length and have nano-sized widths, using Kirchhoff formalism[4,18]. They considered an array of rectangular holes with w =200 nm and l =100 μm in a metallic film with h =100 nm on a dielectric substrate of 450 μm thick undopped silicon, as shown Fig. 4 (a). These THz nano-antennas, acting as resonators in THz frequency range, have the maximum field enhancement of about 150 at the resonance frequency of 0.6 THz, which is $\sim\lambda_c/(2n_{eff}l)$, where n_{eff} is the effective refractive index of the air-substrate composite. The samples were fabricated by electron beam (e-beam) lithography using a negative photoresist and a single-layer lift-off process (Fig. 4 (a)). Shown in Fig. 4 (c-d) are normalized amplitude spectra for two periods of 100 μm and 30 μm. For the 30 μm period sample, the normalized amplitude increases to over 90% at the resonance with the hole coverage ratio of only 0.6%. The field enhancement is therefore over 150, calculated by the Kirchhoff integral formalism. Increasing the period to 100 μm increases the field enhancement only slightly, suggesting that the antenna cross-section of each slot antenna on Si substrate is about ~100 μm x 30 μm.

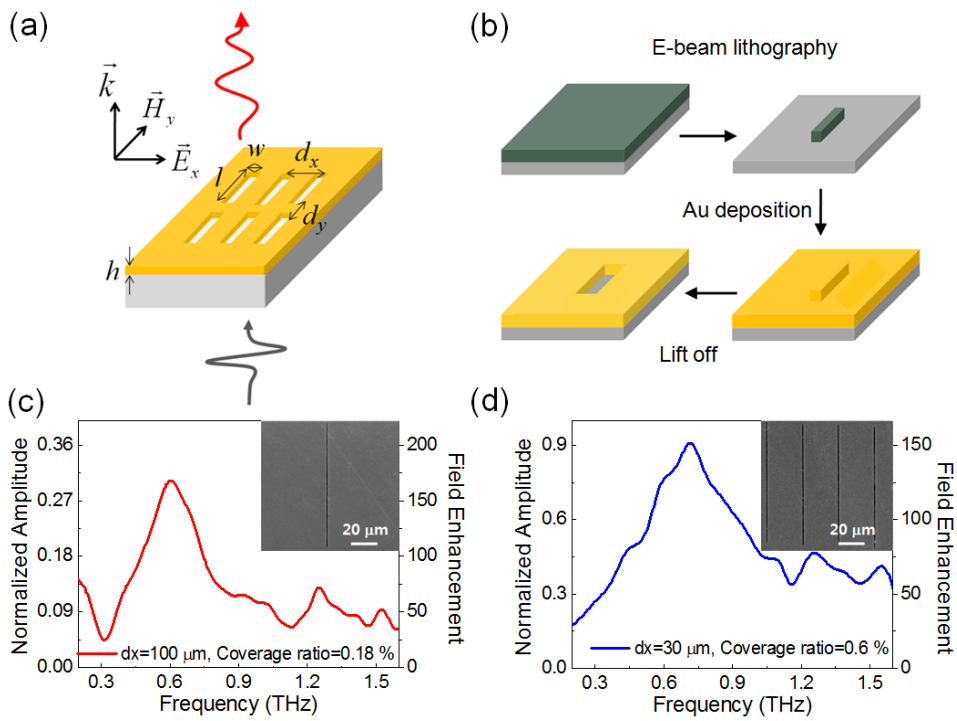

Fig.4. (a) Schematic of an array of rectangular holes. (b) THz nanoantennas are fabricated by e-beam lithography using negative type of photoresist patterning. (c) Normalized transmitted amplitude through an array of nanoantennas with l =100 μm, w =200 nm, and d_x =100 μm and d_y =110 μm. (d) The same as (c) except d_x =30 μm. Inset displays SEM images of the samples (adopted from ref. [4]).

Chapter 3

Lactose Molecules

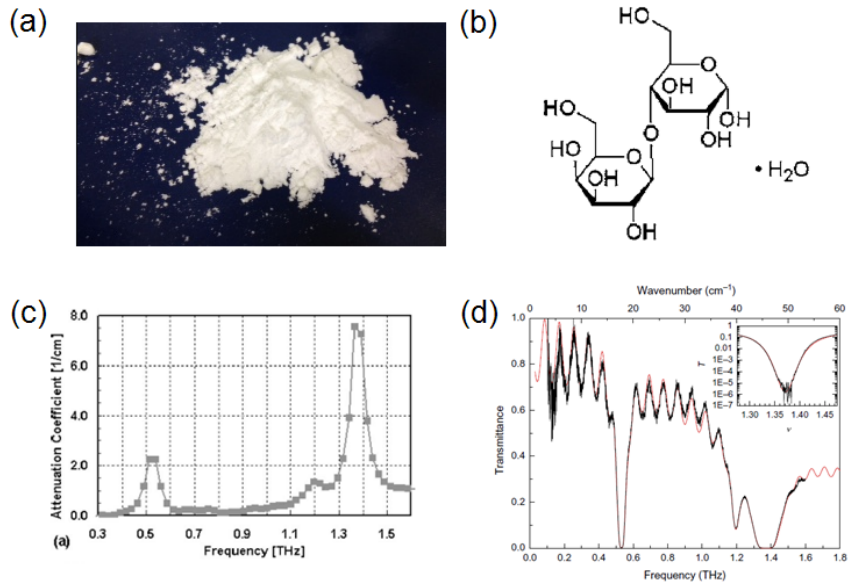

Fig.5. (a) Image of α-lactose monohydrate powder. (b) Molecular structure of α-lactose monohydrate in an aqueous solution. (c) Complete spectrum for the attenuation constant of α-lactose monohydrate diluted to 10% in Teflon powder (adopted from ref. [5]). (d) Transmittance $T(\omega)$ of α-lactose monohydrate for a thickness of 1 mm. Inset: $T(\omega)$ around the absorption feature at 1.369 THz, plotted on a log scale (adopted from ref. [6]).

THz frequencies (0.1 THz~ 10 THz) can be considered as a lower end of the far-infrared region[19]. For this reason, THz spectroscopy is useful for characterizing far-infrared vibrational modes, such as rotational, torsional, phonon, intramolecular modes. In addition, THz spectroscopy can provide informations that are weak in IR vibrational modes such as intermolecular modes.

Lactose $C_{12}H_{22}O_{11}$, consists two anomeric forms, β-D-galactose

ring and α-D-galactose ring, through an oxygen linkage (see Fig. 5 (b))[5]. This structure shows that lactose is capable to fingerprint in THz region because of the potential far-infrared activity of hydrogen bonds with other molecules. As we mentioned before, molecular intra- and intermolecule vibrational modes indicates the materials structure. Therefore, most of chemicals and biomolecules have its own absorption frequencies[24]. Sometimes at certain frequency, some materials might have same frequency, but what I meant is that each material has their own absorption spectra. For example, lactose molecule has absorption frequencies at 0.53, 1.2, 1.37 THz (Fig. 5 (c) and (d)) [5,6,24] while one of the explosive material RDX's shows at 0.72, 1.26, 1.73 THz[24]. Lactose molecules are chosen as a sample because of this optical resonance behavior.

Chapter 4

Experiment

4.1. Sample Fabrication

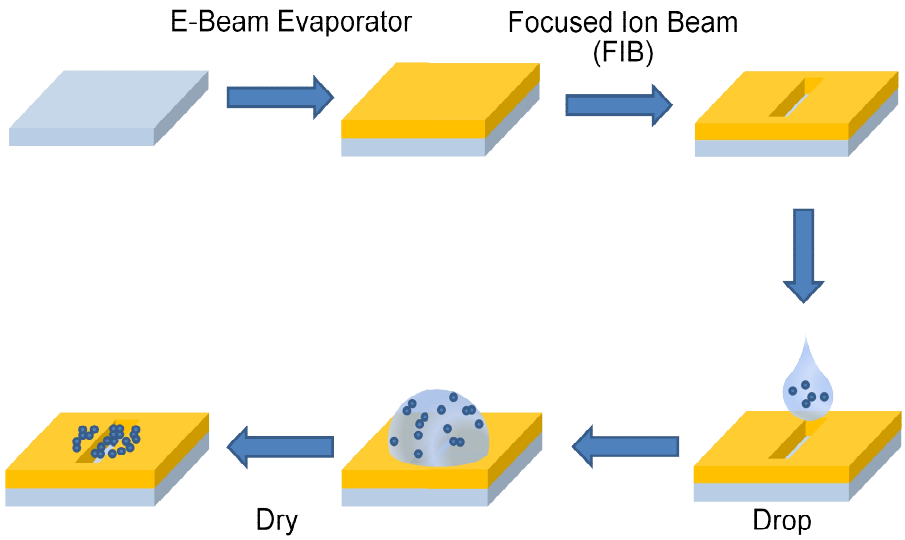

Fig.6. THz nano-slot antenna is fabricated by focused ion beam (FIB) milling process, after depositing gold film with e-beam evaporator. Diluted solution, α-lactose monohydrate in methanol is dropped on the sample and dried in air.

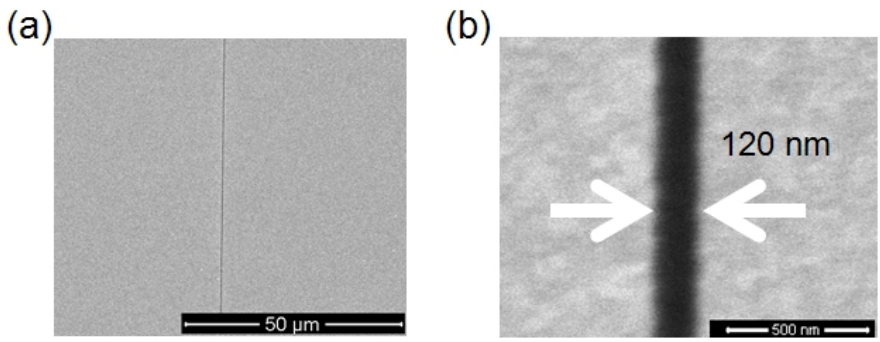

Fig.7. SEM images of a 120nm-width nano-slot antenna after FIB milling process.

Gold film is deposited on the bare quartz substrate. The thickness of the gold film and quartz substrate is 100 nm and 500 μm each. The dimension of the whole sample plate is 1 cm x 1 cm. We punctured various sizes of rectangular holes on gold with focused ion beam. The length of the rectangular-hole (l) is fixed to 150 μm, and the width (w) is 120 nm. After the milling process is finished, we made a diluted solution, α-lactose monohydrate in Methanol 5 mg/mL and 0.01 mg/mL. For the diluted solution of 5 mg/mL case, we dropped 20 μL to pour 0.1 mg on bare quartz and dried it for 15 minutes. Then we repeated the process of dropping the solution and drying in air until the total amount of 2.0 mg was poured on bare quartz. And for the other case (0.01 /mL), we dropped 2 μL to pour 0.02 μg on designed nano-slot antenna and air-dried for 30 minutes. The methanol on nano-slot antennas took more time for drying than on bare quartz. After collecting normalized transmission data with this sample, we repeated the process of dropping the solution and drying in air until the total amount of 0.08 μg was poured on nano-slot antenna.

4.2. THz Time Domain Spectroscopy (THz-TDS)

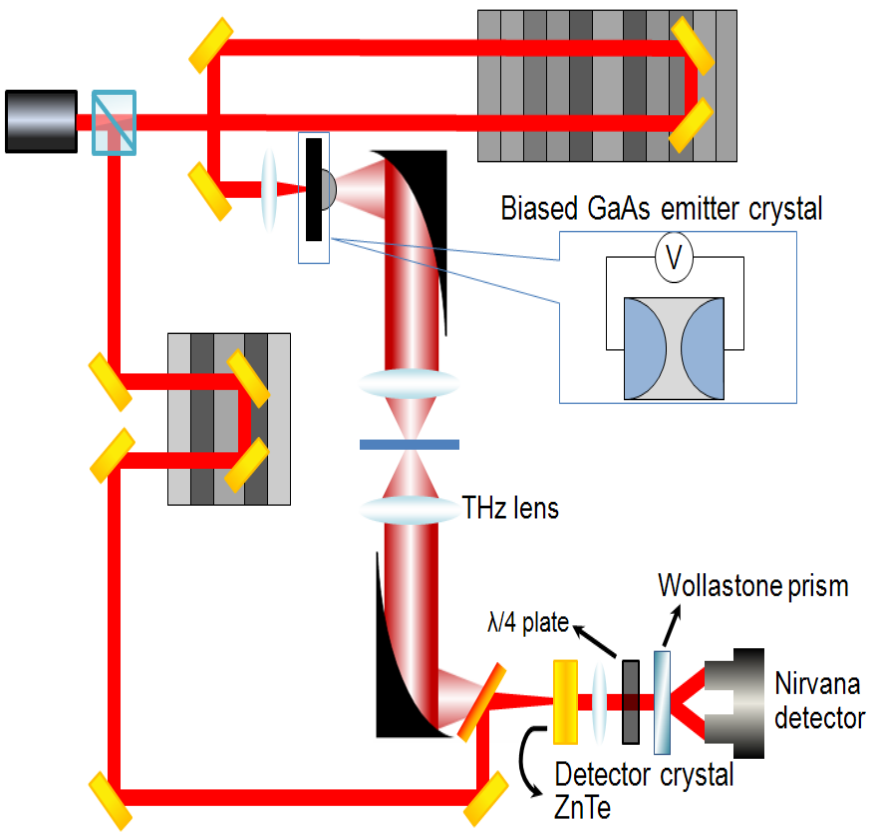

Fig.8. Experimental set-up for measuring the transmitted far field THz wave, using THz lens for tight focusing.

While other techniques enables to measure the amplitude and phase at discrete THz frequencies, time-domain spectroscopy can additionally measure the electric field as a function of time, and obtain the spectrum by a Fourier transform of the time domain data. Terahertz time-domain spectroscopy (THz-TDS) is used to measure the far field enhancement for various samples.

The experimental setup is shown in Fig. 8. We use Ti:Sapphire oscillator as a laser source, generating pulses of 130 fs duration, centered at a wavelength of 780 nm with a repetition rate of 100 MHz. The average power output from the laser is 600 mW. The output from the oscillator is split into two arms by a beam splitter. One is used as pump beam, and the other part is used as probe beam.

As the pump beam passes through a 3 kV/cm biased semi-insulating GaAs emitter, a single-cycle THz source is generated. The hemisphere silicon lens attached on the emitter enables to collect and guide the THz pulse with two parabolic mirrors. Two THz lens are located between the parabolic mirrors, whose focal lengths are 45 mm. THz lenses focus the beam size diameter about 1.5 mm, which is able to detect transmission through single THz nano-slot antenna. The sample is located at the THz focus center, and the transmitted THz wave through a sample is guided to the detection part.

EO detection method is used to measure the THz domain signals.

EO detection is based on a second-order nonlinear response of polarization in an EO material to an applied electric field[18,19]. A refractive index of the EO material is proportionally changed by the THz electric field. The birefringence causes a polarization change of the optical probe pulse that travels through the EO detection crystal. After the detection crystal, the probe beam passes through a quarter-wave plate which is oriented such that the originally linear polarization of the probe beam becomes circular. A signal proportional to the THz electric field is obtained by measuring the difference in the energy of two orthogonal polarization direction beams with a Wollaston prism and two photodiodes. For EO detection, zincblende crystals such as ZnTe and GaP are often used. By selecting the orientation of the detection crystal, it is possible to choose which component of the THz electric field vector the EO detection setup is sensitive to.

Chapter 5

Result

5.1. Absorption Properties

To see the effect of the absorbance of nano-slot antenna, we first detected the absorbance of pure lactose material, and secondly observed the absorbance of lactose on nano-slot antenna. By comparing the absorption coefficient and absorption energy per molecule of these two experimental data, we can recognize how nano-antenna can absorb lactose sensitively.

5.1.1. Experimental Data

By Fourier transforming the time domain data, transmitted amplitude spectra for our sample, $E_{sam}(\omega)$, are obtained with phase information intact. For normalization of the measured spectrum, we use a reference signal, $E_{ref}(\omega)$, for the bare quartz after passing through 1 mm by 1 mm metal aperture. We define the normalized (transmitted) amplitude [T] against the aperture field as the squared ratio between two measured amplitudes,

$$T = |E_{sam}(\omega)/E_{ref}(\omega)|^2. \quad (14)$$

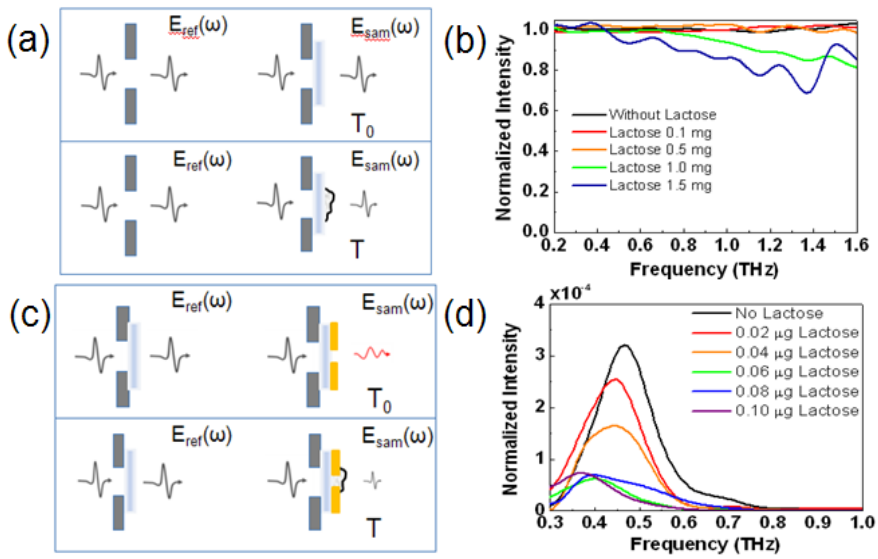

Fig.10. (a) Schematics of a reference aperture and bare quartz, and lactose on a bare quartz. (b) Schematics of a reference aperture and nano-slot antenna with substrate (bare quartz), and lactose on a sample. (c) Normalized transmitted intensity through lactose on bare quartz. (d) The same as (c) except nano-slot antenna sample is used instead of bare quartz.

Experimental results, shown in Fig. 10 (c) and Fig. 10 (d), are the normalized intensity spectra for lactose on bare quartz and on nano-slot antenna with width w =120 nm, length l =150 μm and thickness t =100 nm. For the bare quartz case, as the lactose amount increases the more absorption happens at frequency 0.55 THz and 1.37 THz. This result follows the previous data of other studies' experimental result which shows that lactose has absorption frequency (see Fig. 5 (c) and Fig. 5 (d)). For the other case, lactose on nano-slot antenna case, the antenna's

resonance is designed to have a resonance at 0.6 THz, which is around 0.55 THz. In this case, as the amount of lactose increases normalized intensity decreases until it reaches to 0.06 μg. Because the normalized intensity is similar from 0.06 μg to 0.10 μg, we can assume that lactose is saturated inside the antenna. Both cases of T, bare quartz and nano-slot antenna, are defined to be T_0 which has no lactose on the sample. When lactose 1.5 mg is on bare quartz at 0.55 THz, 7% of the normalized intensity is reduced compared to T_0. On the other hand, lactose 0.08 μg is on nano-slot antenna, 72% of the normalized intensity is reduced at 0.55 THz. From both experimental data, we can see that even though there is 1/20,000 of lactose on the nano-slot antenna, normalized intensity is 11 times more reduced. Thus, lactose on nano-slot antenna absorbs more energy than lactose on bare quartz.

5.1.2. Absorption Coefficient

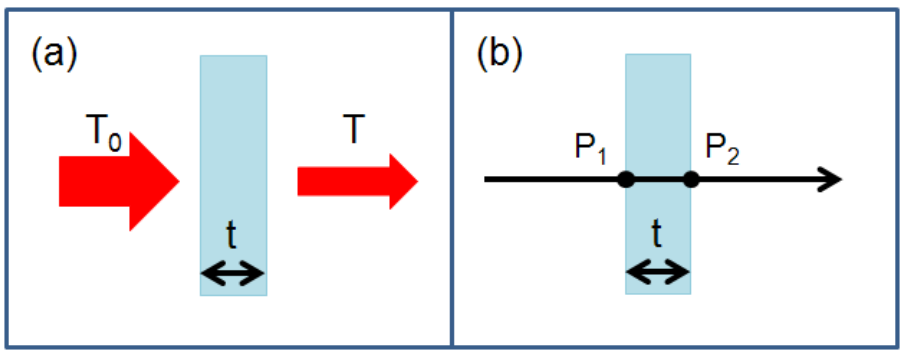

Fig.9. (a) Diagram of absorption of a beam of light as it travels through a material of width t . (b) Illustrating the formula (2) (abopted from ref. [10]).

Before we look through the experimental data, the definition of absorption coefficient is required. Absorption coefficient is a quantity that characterizes how easily a material or medium can be penetrated by a beam of light[9,10,25]. By deriving this constant, we will draw out the factor which indicates the amplitude of the wave decreased exponentially with distance. This means that as the wave progresses, the energy of the wave is absorbed by the medium.

The variation of the space-dependent parts of a complex monochromatic electromagnetic field of frequency ω along each ray in the beam would be given by the formula

$$E_2 = E_1 e^{ik_0 \tilde{n} t} \quad , \quad H_2 = H_1 e^{ik_0 \tilde{n} t}, \qquad (2)$$

where $k_0=\omega/c$, is the free-space wave number and l is the distance between two typical points P_1 and P_2 on the ray (Fig. 9); E_1 and E_2 are the space-dependent parts of the electric fields at the points P_1 and P_2, respectively. H_1 and H_2 are the space-dependent parts of the magnetic fields at these points. Suppose next that the medium is weakly absorbing. Formally, absorption may be taken into account by replacing the real refractive index n by a complex one, which we denote by $\tilde{n}$,

$$\tilde{n}=n+i\kappa \qquad (3)$$

where κ, just like n, is a real constant. The constant is usually called the attenuation index of the medium. We identify the intensity of the field with the absolute value of the Poynting vector,

$$I=\left|<\vec{S}>\right|, \qquad (4)$$

$$<\vec{S}>=\frac{1}{2T'}\int_{-T'}^{T'}\frac{c}{4\pi}\left(\vec{E}\times\vec{H}\right)dt, \qquad (5)$$

$$=\frac{c}{16\pi}\left(\overrightarrow{E_0}\times\overrightarrow{H_0}^{*}+\overrightarrow{E_0}^{*}\times\overrightarrow{H_0}\right) \qquad (6)$$

$$\cong\frac{c}{8\pi}Re\left(\overrightarrow{E_0}\times\overrightarrow{H_0}^{*}\right), \qquad (7)$$

Thus,

$$I=\left|\frac{c}{8\pi}Re\left(\vec{E}\times\vec{H}^{*}\right)\right|=\frac{c}{4\pi}\left|<\vec{E}\times\vec{H}>\right|, \qquad (8)$$

$$I_2=I_1e^{-\alpha t}, \qquad (9)$$

where the constant

$$\alpha=2k_0\kappa \qquad (10)$$

is called the absorption coefficient of the medium. Formula (9) is often called Beer's law and is frequently derived by quasi-geometrical arguments of the theory of radiative energy transfer.

For our experiment case, we set

$$I_2 = T \ , \ I_1 = T_0 \ , \tag{11}$$

Formula (9) can be expressed as

$$T = T_0 e^{-\alpha t}, \tag{12}$$

as in Fig. 9 (a). While T and T_0 indicates the measured intensity of transmitted through a layer of material and the incident intensity of transmission, the absorption coefficient can also be written as

$$\alpha = -\frac{1}{t} ln \left(\frac{T}{T_0}\right). \tag{13}$$

When α is huge, it means that the material itself absorbs the intensity of the light dramatically, and it contains a large amount of absorbed energy. On the other hand, when α is small enough, the material is relatively transparent to the beam of light by absorbing less energy. Therefore, each material has its own absorption coefficients containing the energy differently from the beam of light.

5.1.3. Experimental Result of Absorption Coefficient

Previously, in section 5.1.2, theoretically we derived the absorption coefficient (α). With the parameters of equation (13), experimental result of α can be achieved. For the bare quartz case, T_0 =1 and T =0.93. The thickness of Lactose can be calculated from its molar mass (g/mol), amount (g), density (g/cm^3), and distributed area (cm^2). We can use its density, molar mass, and Avogadro's number to get the value of volume per molecule,

$$\text{volume per molecule}(\text{cm}^3) = \left(\frac{\text{density } (^{\text{g}}/_{\text{cm}^3})}{\text{molar mass (g/mol)}} \times \text{Avogadro's number } (\frac{1}{\text{mol}})\right)^{-1}.$$

If we divide number of molecules,

$$\text{number of molecules} = \frac{\text{the amount of Lactose (g)}}{\text{molar mass (g/mol)}} \times \text{Avogadro's number } (\frac{1}{\text{mol}}),$$

to its distributed area (cm^2), number of molecules per area (1/cm^2) is obtained. Multiplying the values of volume per molecule (cm^3) and number of molecules per area (1/cm^2) is equivalent to the thickness of lactose material, which is on the bare quartz substrate. By following this method with the parameters from chart 1, we can figure out the thickness of lactose 1.5mg is t =12.54 μm. In equation (13), we put the

values of T_0 =1, T =0.93 and t =12.54 μm to know that the α of the lactose on bare substrate is α_{bare}=54.95.

Molar mass	342. 30 g/mol
Density	1.525 g/cm^3
Avogadro's number	6.20×10^{-23} /mol
Distributed area	14.15 cm^2

Chart.1. Properties of Lactose molecules (absopted from ref. [26])

For the nano-slot antenna case, the normalized intensity reduction is saturated at 0.06 μg, 0.08 μg, and 0.10 μg. Therefore, we can assume that the thickness is 100 nm. We can compute the absorption coefficient $\alpha_{nanoslot}$= 1.27×10^5 similarly from the bare quartz case by inserting T_0=1.29×10^{-4}, T =3.61×10^{-5} and t =100 nm.

α_{bare} is about 1/2000 of $\alpha_{nanoslot}$. Lactose molecules on the nano-slot antenna hold more energy from the incident beam of light than on bare quartz.

5.1.4. Absorbed Energy per Molecule

As we identified that the intensity of the field with the absolute value of the Poynting vector in section 5.1.2, the intensity is the energy per unit time, per unit area. T is a normalized value of the intensity. To obtain the effect of absorbed energy, we calculate the difference of T_0 and T and divide the nanoslot antenna's case to bare quartz case,

$$(T_{0nanoslot} - T_{nanoslot})/(T_{0bare} - T_{bare}).$$

On the other hand, we define ξ as the value of energy per volume (V), so $\xi \bowtie V$ means total energy (E). However, the volume of lactose in nano-slot and on bare quartz differs from its thickness. If we divide the total energy of nano-slot antenna case ($E_{nanoslot}$) to the total energy of bare quartz case (E_{bare}), the distributed area will be factored out. This could be rewritten into $(\xi_{nanoslot} \times t_{nanoslot})/(\xi_{bare} \times t_{bare})$, and this should match with $(T_{0nanoslot} - T_{nanoslot})/(T_{0bare} - T_{bare})$.

Nevertheless, it is not equivalent. The reason is that values of T_0 in the case of bare quartz and nano-slot antenna are not the same. Therefore, we have to consider coverage ratio (β)[18]. Coverage ratio is the portion of nano-slot antenna's hole area to aperture area. This ratio intends the relative amplitude of $T_{0nanoslot}$ when we set T_{0bare} to 1. As we get the value of energy per volume of each case and its coverage ratio, the factor of $\xi_{nanoslot}/\xi_{bare}$,

$$\xi_{nanoslot} / \xi_{bare} = \frac{(T_{o\,nanoslot} - T_{nanoslot})/t_{nanoslot}}{(T_{o\,bare} - T_{bare})/t_{bare}} \times 1/\beta \qquad (15)$$

is identified as 5.42×10^4.

Specifically, we have obtained the result that the lactose molecule inside nano-slot antenna absorbs about 54,000 times more than without the antenna.

5.2. Control Experiment

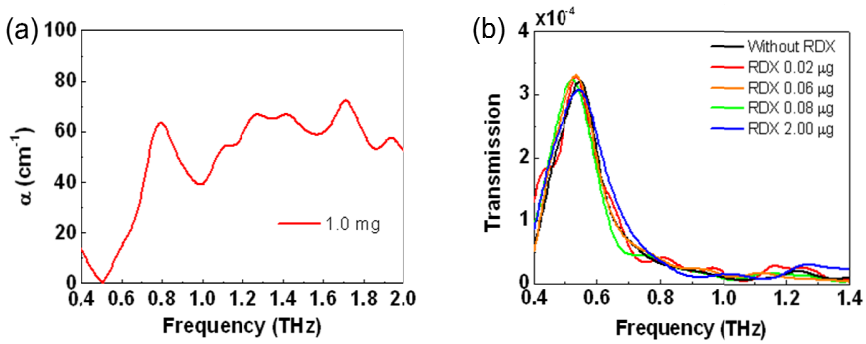

Fig.11. (a) Absorption coefficient of RDX molecule in THz range. (b)Normalized transmitted intensity through RDX on 120nm-width nano-slot antenna, l =150 μm, t = 100 nm.

Fig. 11 (a) shows the absorption coefficient of RDX which has the resonance around 0.8 THz[19]. In Fig. 11 (b), it shows the normalized transmission spectra of RDX on nano-slot antenna array. The nano-slot antenna array is designed to have a resonance frequency at 0.6 THz, with w =120 nm, l =150 μm, and t =100 nm. Although the amount of RDX increases on the antenna array, there is no change of the transmission. No difference of transmission also means that there is no absorption of the material. Thus, this experiment result indicates that the material cannot be detected when the resonance of its absorption and nano-slot antenna are different.

Chapter 6

Summary

THz frequencies matches the low-frequency vibration and the vibration modes of weak interactions, such as hydrogen bonds, THz spectroscopy constitutes a unique tool for studying various molecules and materials whose molecular and/or crystal structures are stabilized by these weak interactions. Lactose molecule suits in this case.

SERS, SEIRA, and CEIRA were introduced as an improved method of detecting single-molecules than just depending on its vibrational modes in IR region. Metallic optical antennas were strongly suggested as a materials' sensor due to its tunable and sharp resonance. For a quantitative analysis, we designed nano-slot antenna which has a negative structure. Since we have studied nano-slot antenna can occur field enhancement in a certain frequency, we put lactose molecules inside. The antenna's absorption resonance is designed to match with lactose molecule's intervibrational modes.

When THz waves go through lactose molecule which is inside the nano-slot antenna, absorption coefficient and absorbed energy per molecule shows an increase 200,000%, 5,000,000% each than without nano-slot antenna. This shows that with THz spectra and nano-slot antenna, the antennas can detect the small amount of molecules and/or materials of interest when the resonances are matched with the antennas. Because of its sensitivity, nano-slot antenna can be used as a tool for identifying materials.

Reference

1. Garcia-Vidal, F. J. et al. Transmission of Light through a Single Rectangular Hole. Physical Review Letters 95, 103901 (2005).
2. Seo, M. A. et al. Near field imaging of terahertz focusing onto rectangular apertures. Opt. Express 16, 20484-20489 (2008).
3. Seo, M. A. et al. Terahertz field enhancement by a metallic nano slit operating beyond the skin-depth limit. Nat Photon 3, 152-156 (2009).
4. Park, H. R. et al. Terahertz nanoresonators: Giant field enhancement and ultrabroadband performance. Applied Physics Letters 96, 121106-121103 (2010).
5. Brown, E. R. and J.E. Bjarnason, On the strong and narrow absorption signature in lactose at 0.53 THz. Applied Physics Letters 90, 061908 (2007)
6. Roggenbuck, A. et al. Coherent broadband continuous-wave terahertz spectroscopy on solid-state samples. New Journal of Physics. 12, 043017 (2010).
7. Born, M. et al. Electromagnetic theory of propagation, interference and diffraction of light. (Cambridge university press, 2003).
8. Fowles, G. R. et al. Introductrion to modern optics. (Dover Publications, Inc., 1975.)
9. Jackson, J. D. Classical Electrodynamics Third ed. (John Wiley & Sons, Inc., 1998).
10. Born, M. and E. Wolf, Principles of Optics Seventh ed. (Pergamon

Press, 1964).

11. Novotny, L. and B. Hecht, Principles of Nano-Optics. (Cambidge university press, 2006).

12. Altug, H. et al. Ultra-sensitive vibrational spectroscopy of protein monolayers with plasmonic nanoantenna arrays. PNAS 106, 19227 (2009).

13. Giessen, H. et al. Hole-Mask Colloidal Nanolithography for Large-Area Low-Cost Metamaterials and Antenna-Assisted Surface-Enhanced Infrared Absorption Substrates. ACS Nano 6, 979 (2012)

14. Osawa, M. et al. Dynamic processes in electrochemical reactions studied by surface-enhanced infrared absorption spectroscopy (SEIRAS). Bull. Chem. Soc. Jpn. 70, 2861 (1997)

15. Altug, H. ,G. Shvets, and et al. Fano-resonant asymmetric metamaterials for ultrasensitive spectroscopy and identification of molecular monolayers. Nature materials 11, 69 (2012)

16. Nie, S. M. and S.R. Emory, Probing Single Molecules and Single Nanoparticles by Surface-Enhanced Raman Scattering. Science 275, 1102 (1997)

17. Zhang, X. et al, Split ring resonator sensors for infrared detection of single molecular monolayers. APL 95, 043113 (2009)

18. Kim, D. S., Y. M. Bahk, and P. C. M. Planken, Terahertz near-field: imaging and field enhancements.

19. Ueno, Y. and K. Ajito, Analytical Terhertz Spectroscopy. Analytical Sciences 24, 185 (2008)

20. Saito, S. et al, First Principles Caculation of Terahertz Vibrational Modes of a Disacchride monohydrate Crystal of Lactose. Jpn. J. Appl. Phys. 45, L1156-L1158 (2006)

21. Shen Y.C. et al, Chemical mapping using reflection terahertz pulsed imaging. Semicond. Sci. Technol. 20, S254-S257 (2005)

22. Fischer, B. et al, Chemical recognition in terahertz time-domain spectroscopy and imaging. Semicond. Sci. Technol. 20, S246-S253 (2005)

23. Taday, P. F., Applications of terahertz spectroscopy to pharmaceutical sciences. Phil. Trans. R. Soc. Lond. A 362, 351–364 (2004)

24. Federici, J. F. et al. THz imaging and sensing for security applications-explosives, weapons and drugs. Semicond. Sci. Technol. 20, S266-S280 (2005)

25. Fowles, G. R., Introduction to modern optics second ed. (Holt, Rinehart and Winston, 1968)

26. http://en.wikipedia.org/wiki/Lactose

국문 초록

테라 파 (주파수=0.1~10 THz, 파장=0.03~ 3 밀리미터) 영역대의 빛이 나노 슬랏 안테나 안의 유당 (α-lactose monohydrate) 분자들을 통과하였을 때, 유당 분자가 얼마나 많이 그 빛을 흡수하는 지 알아보는 실험이다. 최근 분자 분광학, 표면 플라즈몬 분야에서는 유당 분자가 테라 파 영역 대에서 분자간 진동운동에 의해, 0.53 THz 에서 흡수 주파수를 가지고 있는 것으로 소개되었다. 나노 슬랏 안테나에서 또한 공명 현상이 나타나기 때문에 우리는 유당 분자의 같은 공명을 이룰 수 있는 안테나를 설계했다. 나노 슬랏 안테나는 금속 막에 사각 구멍이 있는 경우를 말하는데, 이 때 파장 이하의 좁은 사각 구멍을 투과하는 빛이 구멍의 길이와 공명을 일으켜, 특정 파장에서 강하게 증폭되는 현상을 보여준다. 증폭된 전기장 안에 있는 유당 분자의 흡수 계수와 분자 당 흡수 에너지가 각각 2천배, 5만배 정도 증가됨을 볼 수 있었다. 따라서, 흡수 주파수를 갖고 있는 물질 혹은 분자크기의 입자를 검출하기 위한 고감도센서로서 나노 슬랏 안테나를 활용할 수 있을 것으로 전망된다.

주요어: 테라 파, 락토즈 분자, 나노슬랏 안테나, 흡수
학 번: 2010-23151